View metadata, citation and similar papers at core.ac.uk

brought to you by CORE

provided by Xiamen University Institutional Repository

Two I_h-symmetry-breaking C_{60} isomers stabilized by chlorination

YUAN-ZHI TAN*, ZHAO-JIANG LIAO*, ZHUO-ZHEN QIAN, RUI-TING CHEN, XIN WU, HUA LIANG, XIAO HAN, FENG ZHU, SHENG-JUN ZHOU, ZHIPING ZHENG, XIN LU, SU-YUAN XIE†, RONG-BIN HUANG AND LAN-SUN ZHENG

State Key Laboratory for Physical Chemistry of Solid Surfaces and Department of Chemistry, College of Chemistry and Chemical Engineering, Xiamen University, Xiamen 361005, China

*These authors contributed equally to this work

†e-mail: syxie@xmu.edu.cn

Published online: 7 September 2008; doi:10.1038/nmat2275

One abiding surprise in fullerene science is that I_h-symmetric buckminsterfullerene C_{60} (ref. 1) (I_h–C_{60} or $^{\#1,812}C_{60}$, the nomenclature specified by symmetry or by Fowler's spiral algorithm[2]) remains the sole C_{60} species experimentally available. Setting it apart from the other 1,811 topological isomers (isobuckminsterfullerenes) is its exclusive conformity with the isolated-pentagon rule[3], which states that stable fullerenes have isolated pentagons. Although gas-phase existence of isobuckminsterfullerenes has long been suspected[4–7], synthetic efforts have yet to yield successful results. Here, we report the realization of two isobuckminsterfullerenes by means of chlorination of the respective C_{2v}- and C_s-symmetric C_{60} cages. These chlorinated species, $^{\#1,809}C_{60}Cl_8$(1) and $^{\#1,804}C_{60}Cl_{12}$(2), were isolated in experimentally useful yields. Structural characterization by crystallography unambiguously established the unique pentagon–pentagon ring fusions. These distinct structural features are directly responsible for the regioselectivity observed in subsequent substitution of chlorines, and also render these unprecedented derivatives of C_{60} isomers important for resolving the long-standing puzzle of fullerene formation by the Stone–Wales transformation scheme[8–11].

Our synthesis followed the classical Krätschmer–Huffman process[12] using CCl_4 or Cl_2 as the chlorine source (see the Methods section), which we used previously in the synthesis of D_{5h}–$C_{50}Cl_{10}$ (refs 13,14). The C_{2v}- and C_s-symmetric C_{60} cages, both stabilized by chlorination, were isolated from the product mixture as **1** and **2**, respectively (Fig. 1). After optimization of the reaction conditions, the weight content of **1** in the toluene extract of the crude product can be improved to 3.5%, which is more than that of D_{5h}–C_{70} (2.6%) and comparable to that of I_h–C_{60} (4.2%) (see Supplementary Information S2, Fig. S2). The yield of **2** is about 10% of **1**. It should be noted that the yields are significantly higher than those of previously reported isolated-pentagon rule (IPR)-violating fullerenes[15,16], and are sufficient for detailed characterization and property investigations.

These novel C_{60} derivatives are soluble in solvents typically used in fullerene studies, including toluene, benzene, chloroform and carbon disulphide. In addition to characterization by ^{13}C nuclear magnetic resonance (NMR), mass spectrometry, infrared and ultraviolet/visible spectroscopies (see Supplementary Information S3, Figs S4–S11 and Tables S2,S3), the crystal structures of **1** and **2** have been determined and are shown in Fig. 1a. The overall symmetry of **1** is C_{2v}, the same as its parent cage, whereas chlorination of the otherwise C_s-symmetric $^{\#1,804}C_{60}$ isomer causes complete loss of its mirror symmetry, producing **2** as a chiral species (Fig. 1a, Supplementary Information S4, Fig. S12). In both **1** and **2**, the chlorine-bonded sp^3-C atoms form a 'belt', splitting the cage into aromatic fragments of C_{10} and C_{42} in **1** and of C_{16} and C_{32} in **2**. The larger portions, C_{42} and C_{32}, are similar to their counterparts in I_h–C_{60} with alternating C=C and C–C bonds, whereas the smaller moieties, C_{10} and C_{16}, structurally resemble the aromatic benzenoid and/or naphthalenoid patches. Such aromaticity contributes to the overall stability of **1** and **2** and serves to rationalize the observed site-specific chlorination of these isomeric cages (see below). The significance of aromatic fragments in contributing to the overall stability of fullerene derivatives has previously been elaborated by Taylor and co-workers in their production of various fullerene derivatives, including hydrides, hydroxides, halides, oxides, alkyl- and arylfullerenes and cycloadducts[17,18].

The most prominent feature of these two isomeric C_{60} cages is the presence of pentagon–pentagon ring fusions, two in $^{\#1,809}C_{60}$ and three in $^{\#1,804}C_{60}$ (Fig. 1). They thus represent the very first examples of C_{60} that violate the well-recognized and widely accepted IPR (ref. 3). Model studies revealed significantly reduced angles between the mean planes of the involved rings (and therefore, enhanced curvature) and reduced aromaticity along the cage surface (see Supplementary Information S5) as a result of the pentagon adjacency. The consequence is at least twofold. First, it explains why releasing the inherent strain of the 'deformed' cages by means of chlorination or possibly other methods is necessary for their stabilization[19]. The stabilizing effect of exo-chlorination of the deformed cages is further supported by density functional computations at the Perdew–Burke–Ernzerhof/double-numerical plus polarization level of theory[20] (see the Methods section and Supplementary Information S4). Compound **1**, for example, is 33.1 kcal mol^{-1} lower in energy than the octachloro derivative of I_h–C_{60}. In addition, the highest occupied molecular orbital–lowest occupied molecular orbital gap of 1.76 eV is larger than that of octachloro I_h–C_{60} (1.41 eV, Supplementary Information S4,

© 2008 Macmillan Publishers Limited. All rights reserved.

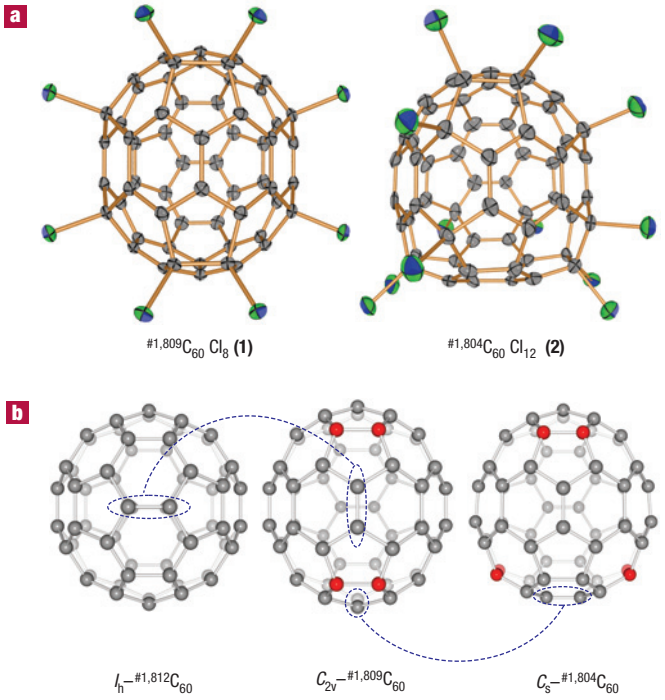

Figure 1 Structures of $^{\#1,809}C_{60}Cl_8$ (1) and $^{\#1,804}C_{60}Cl_{12}$ (2). a, Oak Ridge Thermal Ellipsoid Plot drawings of the crystal structures of **1** and **2**. Thermal ellipsoids are shown at 50% probability level. **b**, Geometries of the three C_{60} isomers optimized by computation. Carbon atoms along pentagon–pentagon fusions are coloured red. The dashed lines indicate the Stone–Wales transformations from C_s–$^{\#1,804}C_{60}$ to C_{2v}–$^{\#1,809}C_{60}$, and eventually to I_h–$^{\#1,812}C_{60}$. Such isomerizations involve successive 90° rotations of a C_2 unit (indicated by blue dashed lines) between two abutting hexagons.

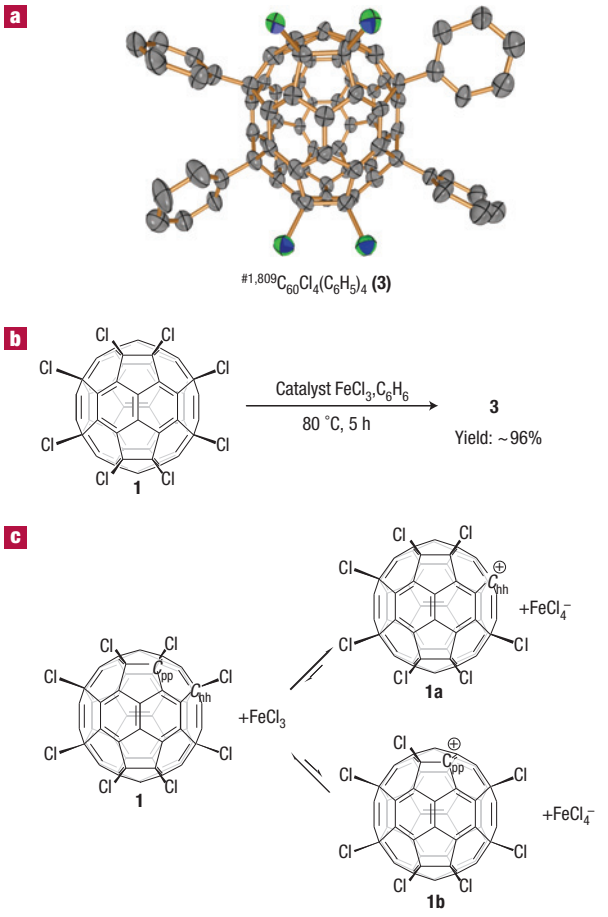

Figure 2 The synthesis of $^{\#1,809}C_{60}Cl_4(C_6H_5)_4$. a, Oak Ridge Thermal Ellipsoid Plot drawing of the crystal structure of $^{\#1,809}C_{60}Cl_4(C_6H_5)_4$. Thermal ellipsoids are shown at 50% probability level; hydrogen atoms are omitted for clarity. **b**, Chemical synthesis of $^{\#1,809}C_{60}Cl_4(C_6H_5)_4$ through a Friedel–Crafts reaction catalysed by $FeCl_3$. **c**, Formation of two possible cationic intermediates $[C_{60}Cl_7]^+$, **1a** and **1b**, anticipated as intermediates in the synthesis of $^{\#1,809}C_{60}Cl_4(C_6H_5)_4$.

Fig. S13). Stabilization of fullerenes by functionalizing their reactive parent cages has also been demonstrated by the fluorination of a C_{58} species featuring a seven-membered ring[21] as well as by the theoretically predicated stability of $C_{60}F_{60}$ (ref. 22). Second, unusual physical properties and chemical reactivity of these novel and more energetic isomers may be expected[23]. Although direct exploration of such isomeric C_{60} cages in the solid state is not yet possible owing to their highly reactive nature, we note that their structural 'deformation' originated from the fusing pentagons is shared by the chlorinated species. The geometry of the sp^3-hybridized C at the pentagon fusion sites, as reflected by the average C–C–Cl bond angles (113.2° in **1** and 112.7° in **2**), deviates more severely from a regular tetrahedron (109.48°) than those of the other sites (111.4° in **1** and 111.2° in **2**) (see Supplementary Information S5). It follows that any unusual properties of the isomeric fullerenes due to pentagon fusion-related 'deformation' might be retained in the chlorinated species, such as site-differentiated chemical transformations.

Indeed, such submissions have been validated subsequently by the regiospecific substitution of the Cl atoms of these unprecedented species. We first attempted classical Friedel–Crafts reactions[24] with $FeCl_3$ as the catalyst (see the Methods section and Supplementary Information S6). A tetra-substituted derivative, $^{\#1,809}C_{60}Cl_4(C_6H_5)_4$ (**3**), was isolated in quantitative yield from the reaction of **1** with benzene under reflux for 5 h (Fig. 2). Longer reaction time did not yield any more extensively substituted species, whereas shortening the reaction time afforded $^{\#1,809}C_{60}Cl_{8-n}(C_6H_5)_n$ ($n = 1$–3) containing fewer phenyl substituents (Supplementary Information S6, Fig. S19). Nevertheless, further transformations of these intermediate species are possible. For example, reacting $^{\#1,809}C_{60}Cl_{8-n}(C_6H_5)_n$ ($n = 1$–3) with toluene in the presence of catalytic $FeCl_3$ produced $^{\#1,809}C_{60}Cl_4(C_6H_5)_n(C_6H_4CH_3)_{4-n}$ ($n = 1$–3) (Supplementary Information S6, Fig. S20); again no more than four Cl atoms are substituted, clearly suggesting their disparate reactivity and the possibility of creating multifunctional materials through site-specific modification of isobuckminsterfullerenes.

Crystallographic studies as well as ^{1}H NMR, mass spectrometry, infrared and ultraviolet/visible spectroscopies (Supplementary Information S6, Figs S15–S18) provide unambiguous evidence for the aforementioned site-specificity in Cl substitution. The molecular structure of **3** is shown in Fig. 2. All four Cl atoms at the hexagon–hexagon (C_{hh}) vertices are replaced by phenyl groups, whereas the four Cl atoms at the pentagon–pentagon (C_{pp}) fusion sites remain intact. In comparison, the reaction of $^{\#1,812}C_{60}Cl_6$, a typical chlorination derivative of I_h–C_{60}, under the same conditions leads to complete replacement of the Cl atoms unless sterically encumbering substituents are used[25–27].

This site-specific reactivity, clearly a result of the unique structure of the IPR-violating C_{60} cage, can be rationalized in

© 2008 Macmillan Publishers Limited. All rights reserved.

terms of the relative stability of the cationic intermediates expected in a Friedel–Crafts reaction. In a typical Friedel–Crafts reaction catalysed by $FeCl_3$, the formation of a carbocation intermediate is usually rate-determining[24]. Our computations show that **1b**, a $^{\#1,809}C_{60}Cl_7^+$ intermediate arising from the heterolytic rupture of a C_{pp}–Cl bond, is 13.3 kcal mol^{-1} less stable than **1a** (Fig. 2c; Supplementary Information S4, Fig. S14), the corresponding intermediate resulting from analogous cleavage of a C_{hh}–Cl bond. This result is in accord with the crystal structure of **1**, in which the C_{hh}–Cl bonds are shown to be longer than the C_{pp}–Cl bonds. We presume that the chlorines of the longer C_{hh}–Cl bonds would be removed more readily, producing **1a** and its subsequent reaction products with benzene or toluene. The greater difficulty of forming carbocations at the C_{pp} sites may also be rationalized in terms of the different pyramidalization angle between C_{hh} and C_{pp} sites: π-orbital axis vector[28] angles at the C_{hh} and C_{pp} sites in $[C_{60}Cl_7]^+$ are 10.47° and 12.12°, respectively (Supplementary Information S4, Fig. S14). It is evident that carbocation **1b** is both energetically and structurally less favoured, and hence the observed non-reactivity at these four sites.

The chlorinated C_{60} isomers also undergo facile reactions with nucleophiles. For example, sodium methoxide reacted with **1** to give an octamethoxylated $^{\#1,809}C_{60}$ in which all eight Cl atoms were replaced (see the Methods section and Supplementary Information S6, Fig. S21). Full substitution with phenylcarbinol, a medicinally significant function, was also achieved (see Supplementary Information S6, Fig. S22), but an analogous reaction with glycine methyl ester produced only partially substituted derivatives (Supplementary Information S6, Fig. S23). Owing to the lack of ^{13}C NMR data, we are unable to determine at the present time whether or not the alkoxy substituents are located at the sites originally occupied by the displaced chlorine atoms. The successful preparation of these novel fullerene derivatives provides a glimpse of the bright future that these new members of the fullerene family may offer in creating multifunctional materials. Our imminent studies are to equip **1** with chromophores or other functional groups for possible applications in immunofluorescence or photovoltaics.

The existence of bare C_{60} cages resulting from dechlorination of **1** or **2** was verified by multistage mass spectrometry, whereby stepwise detachment of Cl was achieved by collision of molecules of **1** or **2** in vacuo with high-energy helium (Supplementary Information S7, Fig. S24). As a representative, the progressive loss of Cl atoms of **1** is shown in Fig. 3, with the eventual formation of a non-chlorinated C_{60} unit. Further fragmentation of this C_{60} unit was difficult, thus opening the possibility of studying its molecular and electronic structures by, for example, photoelectron spectroscopy. However, whether this C_{60} unit maintains the formal C_{2v} symmetry of the isomeric structure is unclear at present.

The existence of a pristine non-I_h C_{60} unit was nevertheless confirmed by thermal dechlorination of $^{\#1,809}C_{60}Cl_8$ (**1**) in a nitrogen atmosphere. Figure 4a shows the applied spray pyrolysis set-up equipped with either a furnace (100–500 °C) or a silicon heater (about 1,200 °C). This set-up enables the dechlorinated products to enter directly into a mass spectrometer or to be collected in toluene for high-performance liquid-chromatography (HPLC) analysis (see the Methods section). The common chlorinated species of I_h–C_{60}, $^{\#1,812}C_{60}Cl_6$, was used for comparative studies. Remarkable abundances of bare C_{60}s were seen in the mass spectra (Fig. 4b,c) of the pyrolysis products of both **1** (furnace temperature 500 °C) and $^{\#1,812}C_{60}Cl_6$ (200 °C). As established by the corresponding HPLC analysis (Fig. 4d), the peak of 720 m/z from $^{\#1,812}C_{60}Cl_6$ dechlorination can be explicitly assigned to I_h–C_{60}. In the case of $^{\#1,809}C_{60}Cl_8$, no trace of I_h–C_{60} was observed in HPLC analysis of the decomposition product(s) obtained at 500 °C (Fig. 4e), although a

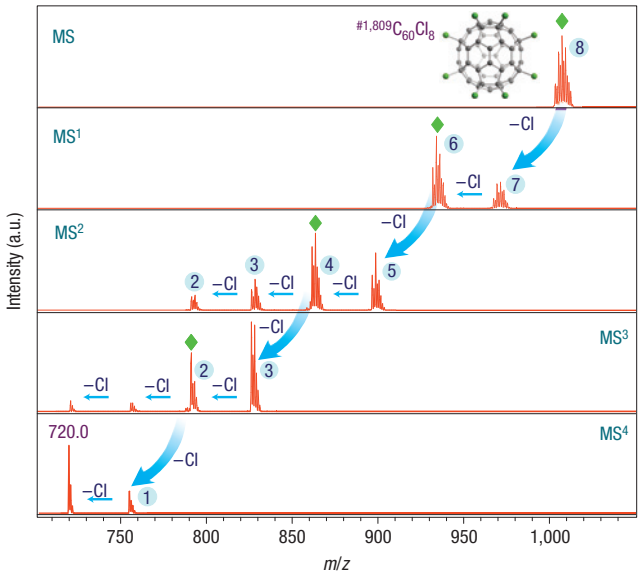

Figure 3 Dechlorination of $^{\#1,809}C_{60}Cl_8$. Multistage mass spectrometry (MS^n, $n = 1$–4) showing the formation of a C_{60} unit with 720 m/z by progressive dechlorination of $^{\#1,809}C_{60}Cl_m$ ($m = 0$–8) (m values are indicated as numbers in blue circles and the species selected for the next stage of mass spectrometry fragmentation are marked with green rhombic symbols). m/z, mass to charge ratio.

720 m/z peak was unmistakably shown in the corresponding mass spectrum (Fig. 4b). This C_{60} unit from the dechlorination of **1** is distinctly different from I_h–C_{60} in terms of symmetry; it may not be entirely unreasonable to assume this 720 m/z peak in Fig. 4b is due to C_{2v}–$^{\#1,809}C_{60}$, directly derived from C_{2v}–$^{\#1,809}C_{60}Cl_8$. As any non-I_h topological isomers of C_{60} are energetically higher and therefore less stable, the essentially featureless HPLC trace may be understood as little soluble species present in the toluene extract owing to aggregation of the reactive isomeric C_{60} units. This insolubility of the decomposed product(s) has subsequently been verified by an independent thermal decomposition experiment and solubility testing of the product mixture.

The fate of the more energetic isomeric C_{60} cages is intriguing[29]. Calculations have shown that of the 1,812 possible topological isomers, $^{\#1,809}C_{60}$ and $^{\#1,804}C_{60}$ are energetically closest to I_h–C_{60} (see Supplementary Information S4, Fig. S12), and the formal transformation (the Stone–Wales transformation) from $^{\#1,804}C_{60}$ to $^{\#1,809}C_{60}$ and from $^{\#1,809}C_{60}$ to $^{\#1,812}C_{60}$ each involves only one 90° rotation of a C_2 unit between two abutting hexagons (Fig. 1b). $^{\#1,809}C_{60}$ and $^{\#1,804}C_{60}$ thus represent two key intermediates immediately preceding the final formation of I_h–C_{60}. Aiming to obtain experimental evidence supporting the Stone–Wales scheme, thermal decomposition of **1** was carried out at 1,200 °C with the use of a silicon heater. HPLC analysis of the toluene-extracted products shows a chromatographic peak at ~83 min (Fig. 4f), similar to the peak of I_h–C_{60} produced thermally from $^{\#1,812}C_{60}Cl_6$ (Fig. 4d). Recognizing the unlikelihood of this peak being any more energetic than non-I_h–C_{60} for reasons elaborated above, the appearance of this peak probably suggests the conversion of the isomeric C_{2v}–$^{\#1,809}C_{60}$ into I_h–C_{60}. However, further spectrometric experiments are required to rule out the possibility of this weak peak at ~83 min being from any species other than I_h–C_{60}.

Aiming to gain further insight into the relationship between I_h–C_{60} and any of its more energetic isomers, the relative concentrations of **1** and I_h–C_{60} present in a series of product

© 2008 Macmillan Publishers Limited. All rights reserved.

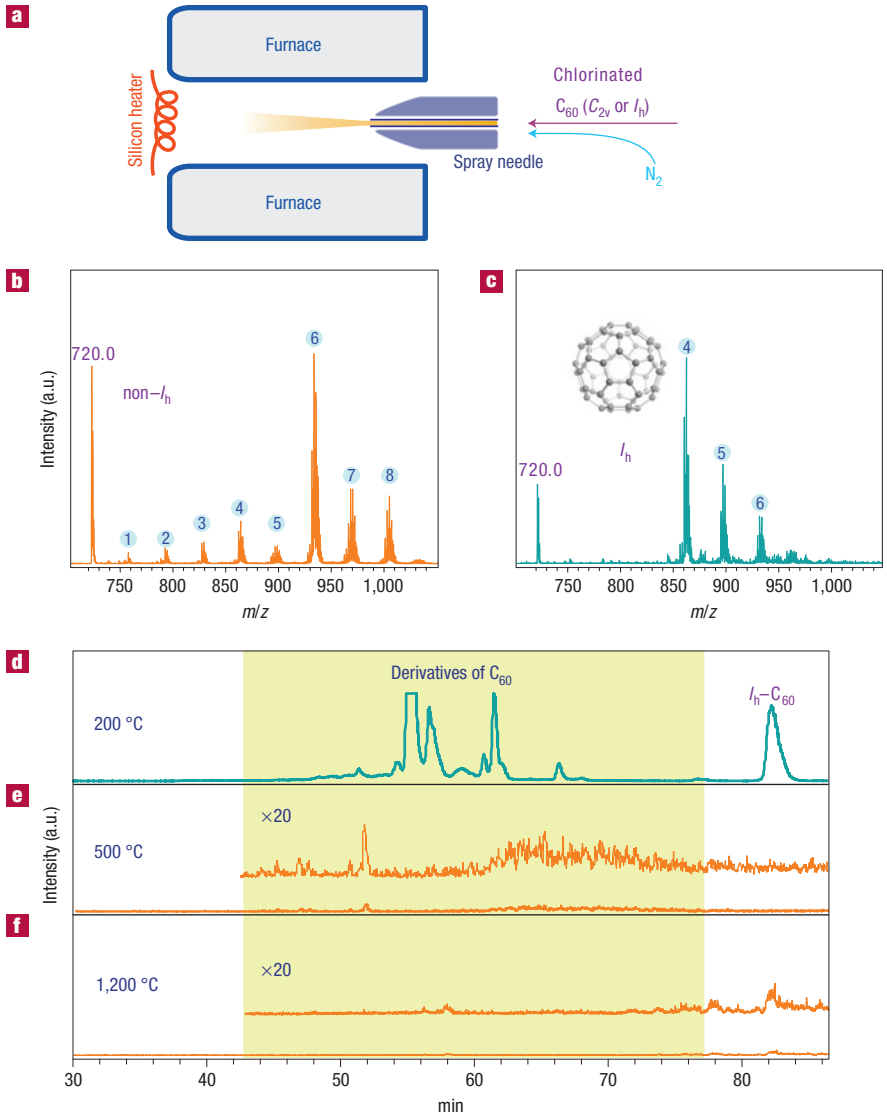

Figure 4 Thermal spray pyrolysis of chlorinated C_{60}s. a, Schematic illustration of the experimental set-up for thermal dechlorination of chlorofullerene by spray pyrolysis. **b**,**c**, Mass spectra of the dechlorinated species $^{\#1,809}C_{60}Cl_n$ (**b**) and $^{\#1,812}C_{60}Cl_m$ (**c**) (*n* and *m* values are marked as numbers in blue circles). The insets show the structure and/or symmetry symbol of the molecule assigned to the peak at 720 *m*/*z*. **d**–**f**, HPLC–mass spectrometry chromatograms (selected ions monitored at 600–1, 500 *m*/*z*) of the toluene-extracted products from spray pyrolysis of $^{\#1,812}C_{60}Cl_6$ at 200 °C (**d**) and $^{\#1,809}C_{60}Cl_8$ at 500 °C (**e**) and 1,200 °C (**f**).

mixtures obtained under different synthetic conditions were analysed. It has been found that the amount of I_h–C_{60} increases linearly as that of $^{\#1,809}C_{60}Cl_8$ decreases (Supplementary Information S8, Fig. S26). Admittedly there may be other mechanism(s) responsible for such an observation, but the current results, in combination with the aforementioned HPLC analysis of the thermal dechlorination products at 1,200 °C, point reasonably to the $^{\#1,809}C_{60}$-to-$^{\#1,812}C_{60}$ isomerization, possibly through the operation of the Stone–Wales transformation scheme. Direct observations of Stone–Wales transformations present in defective carbon nanotubes have recently been reported[30], thus providing supporting evidence for the validity of such a mechanism.

In summary, contrary to the dogma that I_h–C_{60} is the only isolable C_{60} isomer, we show here the existence of two higher-energy isomers of C_{60}, stabilized by chlorination and isolated in yields adequate for any typical fullerene studies. The unique pentagon–pentagon ring fusion featured by these isomers imparts them with interesting chemical reactivity as demonstrated by site-specific replacement of the exohedral Cl atoms. The successful synthesis of these site-differentiated compounds also portends the possibility of creating novel, fullerene-based functional materials. Fundamentally, by studying the thermal dechlorination and transformation of the chlorinated isobuckminsterfullerenes, promising evidence has been obtained in support of the Stone–Wales rearrangement for the formation of I_h–C_{60}. Together, the present results concerning bulk synthesis, regioselective functionalization and mechanistic studies of the unprecedented C_{60} isomers mark a new stage for fullerene research.

METHODS

The carbonaceous soot containing the chlorination derivatives of C_{60} isomers was produced under 0.1974 atm helium and 0.0395 atm carbon tetrachloride (or replaced by 0.0263 atm chlorine gas) in a modified Krätschmer–Huffman

© 2008 Macmillan Publishers Limited. All rights reserved.

arc-discharge reactor equipped with two graphite electrodes, a cathode cylinder block 40 mm (diameter) × 60 mm and an anode rod 8 mm (diameter) × 300 mm. About 5 g h^{-1} soot was produced in the arc-discharge reaction that was supplied with electric power of 33 V and 100 A.

The chlorofullerenes of C_{60} isomers (**1** and **2**), extracted by toluene in a supersonic bath from the carbonaceous soot, were purified by a multistep HPLC process using a Cosmosil Buckyprep column (10 × 250 mm) eluted with toluene. A toluene solution of **1** and a carbon disulphide solution of **2** were slowly vapourized for growing the single crystals of **1** and **2**, respectively.

The functionalizations of **1** were carried out through a Friedel–Crafts reaction and a nucleophilic reaction, respectively. For the Friedel–Crafts reaction, about 5 mg of **1** was dissolved in 12 ml benzene. Catalysed by $FeCl_3$ (12 mg), this solution was refluxed in 80 °C for 5 h to produce **3** in a yield of 96%. The single crystal of **3** was grown from its carbon disulphide solution. The three types of nucleophilic reaction were conducted as follows. (1) 10 ml of toluene solution with 0.1 mg ml^{-1} of **1** was mixed with 10 ml 20 mmol ml^{-1} sodium methoxide solution of methanol at 25 °C for 24 h to generate about 0.8 mg of crude products with significant quantities of $^{\#1,809}C_{60}(OCH_3)_8$. (2) About 1 mg of **1** was dissolved in toluene (4 ml), then mixed with 0.3 ml 0.11 mmol ml^{-1} $C_6H_5CH_2ONa$ solution of toluene at 30 °C for 40 h under stirring. About 1.2 mg of $^{\#1,809}C_{60}(C_6H_5CH_2O)_8$ was produced. (3) About 1 mg of **1** was dissolved in 4 ml toluene/acetate (1:1) mixed solution, followed by adding $NH_2CH_2COOCH_3$ (2 mg). Catalysed by Na_2CO_3 (2 mg), about 0.7 mg of product with significant quantities of $^{\#1,809}C_{60}Cl_4(NHCH_2COOCH_3)_4$ was produced after being refluxed at 70 °C for 24 h.

Thermal dechlorination/isomerization was conducted in a furnace (100–500 °C) or a silicon heater (1,200 °C) of which the temperature was measured by an infrared thermal meter. The pyrolysis product was extracted by toluene, then analysed by HPLC–mass spectrometry with a C18 column (Discovery C18 column, SUPELCO Co.) and a gradient elution of methanol–ethanol–cyclohexane (see Supplementary Information S2, Table S1) at a flow rate of 0.8 ml min^{-1}.

The mass spectra and HPLC chromatograms were obtained on a Bruker Esquire HCT mass spectrometer and an Agilent 1200 series instrument, respectively. The crystallographic data were measured on a Bruker Smart Apex-2000 CCD (charge-coupled device) diffractometer or an Oxford CCD diffractometer. The NMR spectra were acquired on a Bruker AV 400 or a Bruker AV 600 instrument. The infrared and ultraviolet/visible spectra were recorded on a Nicilet 380 Fourier-transform infrared and an ultraviolet/visible spectrophotometer, respectively.

The structural optimizations of all C_{60} isomers and the pertaining derivatives were carried out in terms of the generalized gradient approximation Perdew–Burke–Ernzerhof density functional method with an all-electron double-numerical plus polarization basis set implemented in the $DMol^3$ package.

Received 8 April 2008; accepted 6 August 2008; published 7 September 2008.

References

1. Kroto, H. W., Heath, J. R., O'Brien, S. C., Curl, R. F. & Smalley, R. E. C_{60}: Buckminsterfullerene. *Nature* **318**, 162–163 (1985).
2. Fowler, P. W. & Manolopoulos, D. E. *An Atlas of Fullerenes* (Oxford Univ. Press, Oxford, 1995).
3. Kroto, H. W. The stability of the fullerenes C_n, with $n = 24$, 28, 32, 36, 50, 60 and 70. *Nature* **329**, 529–531 (1987).
4. Yang, S. H., Pettiette, C. L., Conceicao, J., Cheshnovsky, O. & Smalley, R. E. UPS of buckminsterfullerene and other large clusters of carbon. *Chem. Phys. Lett.* **139**, 233–238 (1987).
5. Hunter, J., Fye, J. & Jarrold, M. F. Annealing C_{60}^+: Synthesis of fullerenes and large carbon rings. *Science* **260**, 784–786 (1993).
6. von Helden, G., Gotts, N. G. & Bowers, M. T. Experimental evidence for the formation of fullerenes by collisional heating of carbon rings in the gas phase. *Nature* **363**, 60–63 (1993).
7. Xie, S. Y., Deng, S. L., Huang, R. B., Yu, L. J. & Zheng, L. S. Five isomers of C_{60} generated in microwave plasma of chloroform. *Chem. Phys. Lett.* **343**, 458–464 (2001).
8. Stone, A. J. & Wales, D. J. Theoretical studies of icosahedral C_{60} and some related species. *Chem. Phys. Lett.* **128**, 501–503 (1986).
9. Hawkins, J. M., Nambu, M. & Meyer, A. Resolution and configurational stability of the chiral fullerenes C_{76}, C_{78}, and C_{84}: A limit for the activation energy of the Stone–Wales transformation. *J. Am. Chem. Soc.* **116**, 7642–7645 (1994).
10. Austin, S.J., Fowler, P. W., Manolopoulos, D. E. & Zerbetto, F. The Stone–Wales map for C_{60}. *Chem. Phys. Lett.* **235**, 146–151 (1995).
11. Bettinger, H. F., Yakobson, B. I. & Scuseria, G. E. Scratching the surface of buckminsterfullerene: The barriers for Stone–Wales transformation through symmetric and asymmetric transition states. *J. Am. Chem. Soc.* **125**, 5572–5580 (2003).
12. Krätschmer, W., Lamb, L. D., Fostiropoulos, K. & Huffman, D. R. Solid C_{60}: A new form of carbon. *Nature* **347**, 354–358 (1990).
13. Xie, S. Y. *et al.* Capturing the labile fullerene[50] as $C_{50}Cl_{10}$. *Science* **304**, 699–699 (2004).
14. Chen, Z. F. The smaller fullerene C_{50}, isolated as $C_{50}Cl_{10}$. *Angew. Chem. Int. Ed.* **43**, 4690–4691 (2004).
15. Lu, X. & Chen, Z. F. Curved π-conjugation, aromaticity, and the related chemistry of small fullerenes (<C_{60}) and single-walled carbon nanotubes. *Chem. Rev.* **105**, 3643–3696 (2005).
16. Dunsch, L. & Yang, S. F. Metal nitride cluster fullerenes: Their current state and future prospects. *Small* **3**, 1298–1320 (2007).
17. Taylor, R. Surprises, serendipity, and symmetry in fullerene chemistry. *Synlett* **6**, 776–793 (2000).
18. Taylor, R. Why fluorinate fullerenes? *J. Fluor. Chem.* **125**, 359–368 (2004).
19. Han, X. *et al.* Crystal structures of Saturn-like $C_{50}Cl_{10}$ and pineapple-shaped $C_{64}Cl_4$: Geometric implications of double- and triple-pentagon-fused chlorofullerenes. *Angew. Chem. Int. Ed.* **47**, 5340–5343 (2008).
20. Delley, B. From molecules to solids with the $DMol^3$ approach. *J. Chem. Phys.* **113**, 7756–7764 (2000).
21. Troshin, P. A. *et al.* Isolation of two seven-membered ring C_{58} fullerene derivatives: $C_{58}F_{17}CF_3$ and $C_{58}F_{18}$. *Science* **309**, 278–281 (2005).
22. Jia, J. F., Wu, H. S., Xu, X. H., Zhang, X. M. & Jiao, H. J. Fused five-membered rings determine the stability of $C_{60}F_{60}$. *J. Am. Chem. Soc.* **130**, 3985–3988 (2008).
23. Chen, Z. F. & King, R. B. Spherical aromaticity: Recent work on fullerenes, polyhedral boranes, and related structures. *Chem. Rev.* **105**, 3613–3642 (2005).
24. Solomons, T. W. G. & Fryhle, C. B. *Organic Chemistry* 8th edn 672–673 (Wiley, New York, 2004).
25. Avent, A. G. *et al.* The structure of $C_{60}Ph_5Cl$ and $C_{60}Cl_5H$, formed via electrophilic aromatic substitution. *J. Chem. Soc. Chem. Commun.* **1994**, 1463–1464 (1994).
26. Birkett, P. R. *et al.* Arylation of [60]fullerene via electrophilic aromatic substitution involving the electrophile $C_{60}Cl_6$: Frontside nucleophilic substitution of fullerenes. *J. Chem. Soc. Perkin Trans. 2.* **1997**, 1121–1125 (1997).
27. Hirsch, A. & Brettreich, M. *Fullerenes: Chemistry and Reactions* 279–282 (Wiley–VCH, Weinheim, 2005).
28. Haddon, R. C. π-electrons in three dimensions. *Acc. Chem. Res.* **21**, 243–249 (1988).
29. Goroff, N. S. Mechanism of fullerene formation. *Acc. Chem. Res.* **29**, 77–83 (1996).
30. Suenaga, K. *et al.* Imaging active topological defects in carbon nanotubes. *Nature Nanotechnol.* **2**, 358–360 (2007).

Supplementary Information accompanies the paper at www.nature.com/naturematerials.

Acknowledgements

We gratefully acknowledge helpful discussions with R. F. Curl, Y. D. Li, L. B. Gan, Y. L. Li, G. M. Blackburn and N. F. Zheng. We thank Y. Q. Feng for HPLC support; H. Y. Huang, J. L. Ye, Q. He, L. Zhang, J. M. Li, W. Z. Wen and Y. S. Zhou for experimental support; and G. M. Blackburn for revising the English of the manuscript. This work was supported by the NNSF of China (grant nos 20525103, 20531050, 20721001, 20571062, 20425312) and the 973 Program (grant no. 2007CB815301).

Author information

Reprints and permission information is available online at http://npg.nature.com/reprintsandpermissions. Correspondence and requests for materials should be addressed to S.Y.X.

© 2008 Macmillan Publishers Limited. All rights reserved.